Angular momentum of light in an optical nanofiber

Fam Le Kien,[1,*] V. I. Balykin,[1,2] and K. Hakuta[1]
[1]*Department of Applied Physics and Chemistry, University of Electro-Communications, Chofu, Tokyo 182-8585, Japan*
[2]*Institute of Spectroscopy, Troitsk, Moscow Region 142092, Russia*
(Received 23 January 2006; published 30 May 2006)

We show that light confined in a circularly polarized fundamental mode of a nanofiber has a finite angular momentum, with both spin and orbital components. We derive exact analytical expressions for the angular momentum and its spin and orbital components. We show that the spin component is dominant when the fiber radius is small or large compared to the light wavelength. For intermediate fiber radii, a substantial orbital component appears, which is absent in the two limits mentioned above. The orbital component is maximized when the fiber radius is about one-fourth of the light wavelength.

DOI: 10.1103/PhysRevA.73.053823 PACS number(s): 41.20.Jb, 42.60.Jf, 42.81.−i

I. INTRODUCTION

Electromagnetic radiation carries both energy and momentum. An interaction between radiation and atoms inevitably involves an exchange of momentum. Such an exchange can involve either linear momentum or angular momentum. This leads to radiation forces and torques, and often has mechanical consequences. Spectacular results have been obtained in manipulation and control of motion and temperature of free atoms by radiation forces [1]. However, most of the treatments of the mechanical effects of radiation on atoms have been concerned almost exclusively with the linear momentum to control the *translational* motion of atoms [2].

Recently, there has been a growing recognition of the potential of the orbital angular momentum associated with certain types of laser lights to control the *rotational* motion of atoms and ions [3,4]. It has been shown that Laguerre-Gaussian [5–7] and Bessel [8] light beams carry orbital angular momentum associated with the azimuthal-phase dependence of the field distribution. Such orbital angular momentum can be transferred to the center-of-mass motion of atoms through the atom-field interaction [3,4]. Certain beams with no phase singularity, such as focused elliptical Gaussian beams, can also possess orbital angular momentum [9]. A number of experiments have demonstrated the influence of orbital angular momentum of light on polarizable matter, leading to interesting features, such as the optical spanner effect [10].

Although angular momentum of light is a fundamental characteristic, it has not been studied well enough. In addition, only a few forms of light beams are known to possess orbital angular momentum. Therefore, it is necessary to extend the study of angular momentum of light and to search for new forms of light beams that possess orbital angular momentum.

A special form of propagating light waves is light in a guided mode of an optical fiber [11]. When the fiber is thin compared to the light wavelength, the field can penetrate deeply into the space outside the fiber, creating an evanescent wave [12,13]. It has been shown that the optical potential generated by the field outside the thin fiber permits the control and manipulation of individual neutral atoms in a microscopic (at subwavelength size) optical dipole trap [12] that is of great importance for various applications in both fundamental and applied physics [14].

In this paper, we study the angular momentum of light in a guided mode of an optical fiber. We show that light confined in a circularly polarized fundamental mode of a nanofiber has a finite angular momentum, with both spin and orbital components.

Before we proceed, we note that, due to recent developments in taper fiber technology, thin fibers can be produced with diameters down to 50 nm [15]. Thin fiber structures can be used as building blocks in future atom and photonic micro- and nano-devices.

The paper is organized as follows. In Sec. II we describe the field in a circularly polarized fundamental guided mode. In Sec. III we present analytical results for the angular momentum of the guided field. In Sec. IV we present numerical results. Our conclusions are given in Sec. V.

II. FIELD IN A CIRCULARLY POLARIZED FUNDAMENTAL GUIDED MODE

We consider a light field propagating in a circularly polarized fundamental mode of a subwavelength-diameter fiber (nanofiber) (see Fig. 1). The frequency, free-space wave number, and free-space wavelength of the light are denoted

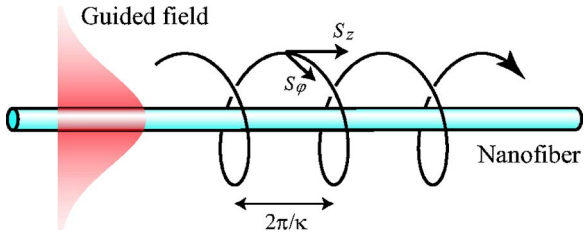

FIG. 1. (Color online) Components and trajectory of the Poynting vector of the field in a circularly polarized fundamental mode of a nanofiber. The period of the trajectory is $2\pi/\kappa$ where $\kappa = S_\varphi / r S_z$.

*Also at the Institute of Physics and Electronics, Vietnamese Academy of Science and Technology, Hanoi, Vietnam.

by ω, $k=\omega/c$, and $\lambda=2\pi/k$, respectively. The thin fiber has a cylindrical silica core, with the radius a and the refractive index n_1, and an infinite vacuum clad, with the refractive index $n_2=1$. For certainty, we assume that the rotation direction of the field polarization around the fiber axis z is counterclockwise. We use the cylindrical coordinates $\{r,\varphi,z\}$.

We represent the electric and magnetic components of the field as $\mathbf{E}=(\boldsymbol{\mathcal{E}}e^{-i\omega t}+\boldsymbol{\mathcal{E}}^* e^{i\omega t})/2$ and $\mathbf{H}=(\boldsymbol{\mathcal{H}}e^{-i\omega t}+\boldsymbol{\mathcal{H}}^* e^{i\omega t})/2$, respectively. The cylindrical components of the envelope vectors $\boldsymbol{\mathcal{E}}$ and $\boldsymbol{\mathcal{H}}$ are given, for $r<a$, by [11]

$$\mathcal{E}_r = i\mathcal{N}\frac{q}{h}\frac{K_1(qa)}{J_1(ha)}[(1-s)J_0(hr)-(1+s)J_2(hr)]e^{i(\beta z+\varphi)},$$

$$\mathcal{E}_\varphi = -\mathcal{N}\frac{q}{h}\frac{K_1(qa)}{J_1(ha)}[(1-s)J_0(hr)+(1+s)J_2(hr)]e^{i(\beta z+\varphi)},$$

$$\mathcal{E}_z = \mathcal{N}\frac{2q}{\beta}\frac{K_1(qa)}{J_1(ha)}J_1(hr)e^{i(\beta z+\varphi)}, \tag{1}$$

and

$$\mathcal{H}_r = \mathcal{N}\frac{\omega\varepsilon_0 n_1^2 q}{\beta h}\frac{K_1(qa)}{J_1(ha)}[(1-s_1)J_0(hr)+(1+s_1)J_2(hr)]e^{i(\beta z+\varphi)},$$

$$\mathcal{H}_\phi = i\mathcal{N}\frac{\omega\varepsilon_0 n_1^2 q}{\beta h}\frac{K_1(qa)}{J_1(ha)}[(1-s_1)J_0(hr)-(1+s_1)J_2(hr)]e^{i(\beta z+\varphi)},$$

$$\mathcal{H}_z = i\mathcal{N}\frac{2q}{\omega\mu_0}s\frac{K_1(qa)}{J_1(ha)}J_1(hr)e^{i(\beta z+\varphi)}, \tag{2}$$

and, for $r>a$, by

$$\mathcal{E}_r = i\mathcal{N}[(1-s)K_0(qr)+(1+s)K_2(qr)]e^{i(\beta z+\varphi)},$$

$$\mathcal{E}_\varphi = -\mathcal{N}[(1-s)K_0(qr)-(1+s)K_2(qr)]e^{i(\beta z+\varphi)},$$

$$\mathcal{E}_z = \mathcal{N}\frac{2q}{\beta}K_1(qr)e^{i(\beta z+\varphi)}, \tag{3}$$

and

$$\mathcal{H}_r = \mathcal{N}\frac{\omega\varepsilon_0 n_2^2}{\beta}[(1-s_2)K_0(qr)-(1+s_2)K_2(qr)]e^{i(\beta z+\varphi)},$$

$$\mathcal{H}_\phi = i\mathcal{N}\frac{\omega\varepsilon_0 n_2^2}{\beta}[(1-s_2)K_0(qr)+(1+s_2)K_2(qr)]e^{i(\beta z+\varphi)},$$

$$\mathcal{H}_z = i\mathcal{N}\frac{2q}{\omega\mu_0}sK_1(qr)e^{i(\beta z+\varphi)}. \tag{4}$$

Here β is the longitudinal propagation constant for the fiber fundamental mode, $h=(n_1^2k^2-\beta^2)^{1/2}$ characterizes the radial dependence of the field inside the fiber, and $q=(\beta^2-n_2^2k^2)^{1/2}$ characterizes the decay of the field outside the fiber. The notation J_n and K_n stand for the Bessel functions of the first kind and the modified Bessel functions of the second kind, respectively. The coefficient $\mathcal{N}$ characterizes the amplitude of the field. For convenience, we have introduced the notation $s=(1/q^2a^2+1/h^2a^2)/[J_1'(ha)/haJ_1(ha)+K_1'(qa)/qaK_1(qa)]$, $s_1=(\beta^2/k^2n_1^2)s$, and $s_2=(\beta^2/k^2n_2^2)s$.

Equations (1)–(4) show that the field possesses not only two individual transverse (radial and azimuthal) components but also a longitudinal (axial) component. The presence of the common phase factor $e^{i\varphi}$ in Eqs. (1)–(4) means that there is an azimuthal-phase dependence. Such a phase dependence is a feature of the field in the fundamental guided mode. Note that the azimuthal-phase dependences of the longitudinal components $\mathcal{E}_z\hat{\mathbf{z}}$ and $\mathcal{H}_z\hat{\mathbf{z}}$ are simple: they contain just the first azimuthal harmonic $e^{i\varphi}$. However, the azimuthal-phase dependences of the transverse components $\boldsymbol{\mathcal{E}}_t=\mathcal{E}_r\hat{\mathbf{r}}+\mathcal{E}_\varphi\hat{\boldsymbol{\varphi}}$ and $\boldsymbol{\mathcal{H}}_t=\mathcal{H}_r\hat{\mathbf{r}}+\mathcal{H}_\varphi\hat{\boldsymbol{\varphi}}$ are rather complicated. The reason is that, in addition to the common phase factor $e^{i\varphi}$ in the expressions for $\mathcal{E}_r$ and $\mathcal{E}_\varphi$ and, similarly, for $\mathcal{H}_r$ and $\mathcal{H}_\varphi$, there is an implicit azimuthal-phase dependence in the nature of the polar basis vectors $\hat{\mathbf{r}}$ and $\hat{\boldsymbol{\varphi}}$. The azimuthal-phase dependences of $\boldsymbol{\mathcal{E}}_t$ and $\boldsymbol{\mathcal{H}}_t$ can be seen more clearly in the spherical tensor basis. This basis consists of the vectors $\mathbf{u}_{\pm1}=\mp(\hat{\mathbf{x}}\pm i\hat{\mathbf{y}})/\sqrt{2}$ and $\mathbf{u}_0=\hat{\mathbf{z}}$. They do not depend on φ. In this basis, an arbitrary vector $\mathbf{V}$ can be expanded as $\mathbf{V}=-V_1\mathbf{u}_{-1}-V_{-1}\mathbf{u}_1+V_0\mathbf{u}_0$,where $V_{\pm1}=\mp(V_x\pm iV_y)/\sqrt{2}=\mp(V_r\pm iV_\varphi)e^{\pm i\varphi}/\sqrt{2}$ and $V_0=V_z$ are the spherical tensor amplitudes. When, we use Eqs. (1)–(4), we can show that the spherical tensor amplitudes $\mathcal{E}_l$ and $\mathcal{H}_l$, where $l=0,\pm1$, contain the azimuthal harmonic $e^{i(l+1)\varphi}$ [16]. Thus, the total field contains three azimuthal harmonics, namely 1, $e^{i\varphi}$, and $e^{2i\varphi}$. As known, a common phase factor $e^{il\varphi}$ results in an orbital angular momentum of $l\hbar$ per photon [3]. Therefore, the guided field may possess an orbital angular momentum, which does not correspond to a single quantum number l but rather a superposition of the three quantum numbers 0, 1, and 2 (see the next section).

An important characteristic of the light propagation is the cycle-averaged Poynting vector

$$\mathbf{S}=\tfrac{1}{2}\,\mathrm{Re}(\boldsymbol{\mathcal{E}}\times\boldsymbol{\mathcal{H}}^*). \tag{5}$$

We denote the axial, azimuthal, and radial components of the vector $\mathbf{S}$ in the cylindrical coordinates by the notation S_z, S_φ, and S_r, respectively. For guided modes of fibers, we always have $S_r=0$. When we insert Eqs. (1)–(4) into Eq. (5), we find that the axial and azimuthal components are given, for $r<a$, by

$$S_z = |\mathcal{N}|^2\frac{\omega\varepsilon_0 n_1^2 q^2}{\beta h^2}\frac{K_1^2(qa)}{J_1^2(ha)}[(1-s)(1-s_1)J_0^2(hr)+(1+s)(1+s_1)J_2^2(hr)],$$

$$S_\varphi = |\mathcal{N}|^2\frac{\omega\varepsilon_0 n_1^2 q^2}{\beta^2 h}\frac{K_1^2(qa)}{J_1^2(ha)}[(1-2s_1+s_1s)J_0(hr)+(1+2s_1+s_1s)J_2(hr)]J_1(hr), \tag{6}$$

and, for $r>a$, by

$$S_z = |\mathcal{N}|^2 \frac{\omega\varepsilon_0 n_2^2}{\beta}[(1-s)(1-s_2)K_0^2(qr) + (1+s)(1+s_2)K_2^2(qr)],$$

$$S_\varphi = |\mathcal{N}|^2 \frac{\omega\varepsilon_0 n_2^2 q}{\beta^2}[(1-2s_2+s_2 s)K_0(qr) - (1+2s_2+s_2 s)K_2(qr)]K_1(qr). \quad (7)$$

The axial component S_z describes the energy flow that propagates along the fiber. The azimuthal component S_φ describes the energy flow that circulates around the fiber. The presence of this flow is due to the existence of the longitudinal components $\mathcal{E}_z$ and $\mathcal{H}_z$ of the field in the fundamental mode. The trajectory of the Poynting vector is described by the spiral curve (r,φ,z) where $r=r_0$ and $d\varphi/dz=S_\varphi/rS_z$ [6]. Since S_z and S_φ do not depend on z, the rotation angle of the Poynting vector is given by $\varphi=\varphi(0)+\kappa z$, where $\kappa=S_\varphi/rS_z$. The period of the trajectory along the z axis is $2\pi/\kappa$. The trajectory is illustrated in Fig. 1.

The propagation power P_z is determined as the integral of S_z over the transverse plane of the fiber, that is,

$$P_z = \int S_z d^2\mathbf{r}. \quad (8)$$

Here we have introduced the notation $\int d^2\mathbf{r}=\int_0^{2\pi} d\varphi \int_0^\infty r\, dr$. When we use the expressions for S_z given in Eqs. (6) and (7), we find $P_z=P_z^{(\mathrm{in})}+P_z^{(\mathrm{out})}$, where

$$P_z^{(\mathrm{in})} = |\mathcal{N}|^2 \frac{\pi a^2 \omega\varepsilon_0 n_1^2}{\beta}\frac{q^2K_1^2(qa)}{h^2J_1^2(ha)}\{(1-s)(1-s_1)[J_0^2(ha) + J_1^2(ha)] + (1+s)(1+s_1)[J_2^2(ha) - J_1(ha)J_3(ha)]\},$$

$$P_z^{(\mathrm{out})} = |\mathcal{N}|^2 \frac{\pi a^2 \omega\varepsilon_0 n_2^2}{\beta}\{(1-s)(1-s_2)[K_1^2(qa) - K_0^2(qa)] + (1+s)(1+s_2)[K_1(qa)K_3(qa) - K_2^2(qa)]\}. \quad (9)$$

The upper indices $^{(\mathrm{in})}$ and $^{(\mathrm{out})}$ indicate the contributions of the field inside and outside the fiber, respectively.

When the fiber material is nonabsorbing and nondispersive, the energy per unit length is given by

$$U = \frac{\epsilon_0}{2}\int n^2 |\boldsymbol{\mathcal{E}}|^2\, d^2\mathbf{r}. \quad (10)$$

Here $n(r)=n_1$ and n_2 for $r<a$ and $r>a$, respectively. When we insert Eqs. (1) and (3) into Eq. (10), we find $U=U^{(\mathrm{in})}+U^{(\mathrm{out})}$, where

$$U^{(\mathrm{in})} = |\mathcal{N}|^2 \pi a^2 \epsilon_0 n_1^2 \frac{q^2K_1^2(qa)}{h^2J_1^2(ha)}\left\{(1-s)^2[J_0^2(ha)+J_1^2(ha)] + (1+s)^2[J_2^2(ha) - J_1(ha)J_3(ha)] + 2\frac{h^2}{\beta^2}[J_1^2(ha) - J_0(ha)J_2(ha)]\right\},$$

$$U^{(\mathrm{out})} = |\mathcal{N}|^2 \pi a^2 \epsilon_0 n_2^2 \left\{(1-s)^2[K_1^2(qa) - K_0^2(qa)] + (1+s)^2[K_1(qa)K_3(qa) - K_2^2(qa)] + 2\frac{q^2}{\beta^2}[K_0(qa)K_2(qa) - K_1^2(qa)]\right\}. \quad (11)$$

We note that the propagation power P_z is related to the energy per unit length U by the formula $P_z=Uv_g$, where $v_g=1/\beta'(\omega)\equiv(d\beta/d\omega)^{-1}$ is the group velocity of light in the guided mode.

III. ANGULAR MOMENTUM OF THE GUIDED LIGHT FIELD

For the electromagnetic field in free space, the linear momentum density is given by $\mathbf{p}_{\mathrm{local}}=\mathbf{S}/c^2$ [17]. For the field in a dielectric medium, there are several formulations for the linear momentum density [18]. The Abraham formulation [19] takes $\mathbf{p}_{\mathrm{local}}=[\mathbf{E}\times\mathbf{H}]/c^2$. This expression is sometimes interpreted as the field-only contribution to the momentum of light. The Minkowski formulation [20] takes $\mathbf{p}_{\mathrm{local}}=[\mathbf{D}\times\mathbf{B}]$. In a recent paper [21], Mansuripur suggested that the momentum of a photon in a dielectric medium has both electromagnetic and mechanical parts and hence is the average of the traditional Abraham and Minkowski forms. The appropriate form remains contentious because the debate has not been settled by experiments. Nevertheless, the Abraham formulation is generally accepted [17,22]. Therefore, in our basic calculations, we adopt the Abraham formulation, that is, we use the definition $\mathbf{p}_{\mathrm{local}}=[\mathbf{E}\times\mathbf{H}]/c^2=\mathbf{S}/c^2$ for the field linear momentum density everywhere in space, inside and outside the fiber. However, the results of the Minkowski expression will also be discussed.

With the above identification for the linear momentum density, the angular momentum density of the electromagnetic field is given by $\mathbf{j}_{\mathrm{local}}\equiv[\mathbf{r}\times\mathbf{p}_{\mathrm{local}}]=[\mathbf{r}\times\mathbf{S}]/c^2$. The integration of $\mathbf{j}_{\mathrm{local}}$ over the cross-sectional plane of the fiber yields the angular momentum per unit length

$$\mathbf{J} \equiv \int \mathbf{j}_{\mathrm{local}}\, d^2\mathbf{r} = \frac{1}{c^2}\int [\mathbf{r}\times\mathbf{S}]\, d^2\mathbf{r}. \quad (12)$$

The only nonzero component of $\mathbf{J}$ is aligned along the fiber axis and is given by

$$J = \frac{1}{c^2}\int rS_\varphi\, d^2\mathbf{r}. \quad (13)$$

Thus, the axial angular momentum J is determined by the azimuthal component S_φ of the Poynting vector. When we substitute the expressions for S_φ given in Eqs. (6) and (7) into Eq. (13), we find $J=J^{(\mathrm{in})}+J^{(\mathrm{out})}$, where

$$J^{(\mathrm{in})} = |\mathcal{N}|^2 \frac{2\pi a^2 \omega\varepsilon_0 n_1^2}{\beta^2 c^2}\frac{q^2K_1^2(qa)}{h^2J_1^2(ha)}[(1+s_1 s)J_1^2(ha) - (1+2s_1+s_1 s)J_0(ha)J_2(ha)],$$

$$J^{(\mathrm{out})} = |\mathcal{N}|^2 \frac{2\pi a^2 \omega \varepsilon_0 n_2^2}{\beta^2 c^2} [(1+s_2 s) K_1^2(qa) - (1+2s_2+s_2 s) K_0(qa) K_2(qa)]. \quad (14)$$

The angular momentum $\mathbf{J}$ can be decomposed into the sum of two terms, $\mathbf{J}=\mathbf{J}_{\mathrm{sp}}+\mathbf{J}_{\mathrm{orb}}$, where

$$\mathbf{J}_{\mathrm{sp}} = \epsilon_0 \int [\mathbf{E} \times \mathbf{A}]\, d^2\mathbf{r} \quad (15)$$

and

$$\mathbf{J}_{\mathrm{orb}} = \mathbf{J} - \mathbf{J}_{\mathrm{sp}} \quad (16)$$

are interpreted as the spin and orbital parts, respectively [17,23]. Here $\mathbf{A}$ is the vector potential in the Coulomb gauge. The decomposition procedure is given in Ref. [23] for the case of a field in free space. We adopt this decomposition for the case of guided modes. However, we recognize that the identification of terms as a spin or orbital is not unique [3].

We write $\mathbf{A}=(\boldsymbol{\mathcal{A}} e^{-i\omega t}+\boldsymbol{\mathcal{A}}^* e^{i\omega t})/2$. In the case considered here, we have $\boldsymbol{\mathcal{A}}=\boldsymbol{\mathcal{E}}/i\omega$. Hence, after time averaging, we obtain $\mathbf{J}_{\mathrm{sp}}=(i\epsilon_0/2\omega)\int[\boldsymbol{\mathcal{E}}\times\boldsymbol{\mathcal{E}}^*]\, d^2\mathbf{r}$. The only nonzero component of $\mathbf{J}_{\mathrm{sp}}$ is aligned along the fiber axis and is given by

$$J_{\mathrm{sp}} = \frac{\epsilon_0}{\omega} \int \mathrm{Im}(\mathcal{E}_r^* \mathcal{E}_\varphi)\, \mathrm{d}^2\mathbf{r}. \quad (17)$$

When we insert Eqs. (1) and (3) into Eq. (17), we find $J_{\mathrm{sp}} = J_{\mathrm{sp}}^{(\mathrm{in})} + J_{\mathrm{sp}}^{(\mathrm{out})}$, where

$$J_{\mathrm{sp}}^{(\mathrm{in})} = |\mathcal{N}|^2 \frac{\pi a^2 \epsilon_0}{\omega} \frac{q^2 K_1^2(qa)}{h^2 J_1^2(ha)} \{(1-s)^2 [J_0^2(ha) + J_1^2(ha)] - (1+s)^2 [J_2^2(ha) - J_1(ha) J_3(ha)]\},$$

$$J_{\mathrm{sp}}^{(\mathrm{out})} = |\mathcal{N}|^2 \frac{\pi a^2 \epsilon_0}{\omega} \{(1-s)^2 [K_1^2(qa) - K_0^2(qa)] - (1+s)^2 [K_1(qa) K_3(qa) - K_2^2(qa)]\}. \quad (18)$$

With the help of Eqs. (14) and (18), we can calculate not only the angular momentum per unit length J and the spin component J_{sp} but also the orbital component

$$J_{\mathrm{orb}} = J - J_{\mathrm{sp}}. \quad (19)$$

The angular momentum per unit length J and its components J_{sp} and J_{orb} are proportional to the number of photons per unit length $N_{\mathrm{ph}}=U/\hbar\omega$. It is convenient to introduce the normalized parameters

$$j \equiv \frac{J}{N_{\mathrm{ph}}} = \frac{J^{(\mathrm{in})} + J^{(\mathrm{out})}}{U/\hbar\omega},$$

$$j_{\mathrm{sp}} \equiv \frac{J_{\mathrm{sp}}}{N_{\mathrm{ph}}} = \frac{J_{\mathrm{sp}}^{(\mathrm{in})} + J_{\mathrm{sp}}^{(\mathrm{out})}}{U/\hbar\omega},$$

$$j_{\mathrm{orb}} \equiv \frac{J_{\mathrm{orb}}}{N_{\mathrm{ph}}} = j - j_{\mathrm{sp}}, \quad (20)$$

which characterize the angular momentum per photon and its spin and orbital components, respectively, in the Abraham formulation.

To get a deep insight into the angular momentum and its spin and orbital components, we approximate these quantities in the limiting cases of small and large fiber radii. First, we consider the limiting case of small fiber radii where

$$a \ll \lambda. \quad (21)$$

In this limit, the light field deeply penetrates into the outside of the fiber. Indeed, when a is small enough, we have the relation $a \ll \lambda \ll q^{-1}$. This yields $q \ll k \cong \beta \sim h < a^{-1}$ or, equivalently, $qa \ll ka \cong \beta a \sim ha < 1$. Hence, we get $s \cong s_2 \cong -1$. Using the above relations as well as the property $\lim_{x\to 0} K_1(x)/K_0(x) = \infty$, we find from Eqs. (11), (14), and (18) that

$$J \cong J^{(\mathrm{out})} \cong J_{\mathrm{sp}} \cong J_{\mathrm{sp}}^{(\mathrm{out})} \cong \frac{4\pi a^2 \varepsilon_0}{\omega} |\mathcal{N}|^2 K_1^2(qa) \quad (22)$$

and

$$U \cong U^{(\mathrm{out})} \cong 4\pi a^2 \epsilon_0 |\mathcal{N}|^2 K_1^2(qa). \quad (23)$$

These approximate expressions give the limiting values $j \cong j_{\mathrm{sp}} \cong \hbar$ and consequently $j_{\mathrm{orb}} \cong 0$ for the case of thin fibers.

Next, we consider the limiting case of large fiber radii where

$$a \gg \lambda. \quad (24)$$

In this limit, the light field is practically confined to the inside of the fiber. Indeed, when a is large enough, we have the relation $a \gg \lambda \sim q^{-1}$. This yields $\beta a \cong k a n_1 > qa \sim ka \gg ha \cong x_0$, where $x_0 \cong 2.405$ is the first zero of the Bessel function $J_0(x)$. Hence, we get $s \cong s_1 \cong -1$. Using these relations as well as the property $J_0(ha) \cong J_0(x_0) = 0$, we find from Eqs. (11), (14), and (18) that

$$J \cong J^{(\mathrm{in})} \cong J_{\mathrm{sp}} \cong J_{\mathrm{sp}}^{(\mathrm{in})} \cong \frac{4\pi a^2 \epsilon_0}{\omega} \frac{q^2}{h^2} |\mathcal{N}|^2 K_1^2(qa) \quad (25)$$

and

$$U \cong U^{(\mathrm{in})} \cong 4\pi a^2 \epsilon_0 n_1^2 \frac{q^2}{h^2} |\mathcal{N}|^2 K_1^2(qa). \quad (26)$$

Hence, we obtain the limiting values $j \cong j_{\mathrm{sp}} \cong \hbar/n_1^2$ and consequently $j_{\mathrm{orb}} \cong 0$ for the case of thick fibers. This result is in agreement with the Abraham expression for the angular momentum of a circularly polarized photon in a dielectric medium [22].

According to the above analysis, in the limits of thin and thick fibers, the orbital angular momentum is vanishing. In these limits, the contributions from the field components $\mathcal{E}_{-1}$ and $\mathcal{H}_{-1}$, which do not depend on φ, are dominant compared to the contributions from the other field components. For intermediate radii, the contributions from the field compo-

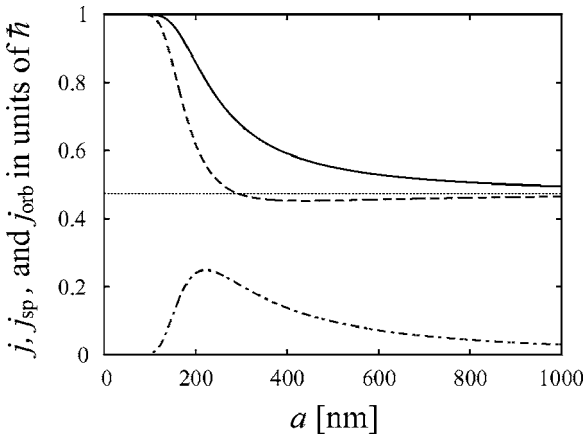

FIG. 2. Total (solid line), spin (dashed line), and orbital (dashed-dotted line) angular momenta per photon in a circularly polarized fundamental mode as functions of the fiber radius. The limiting value $\hbar/n_1^2$ is shown by the dotted line. The light wavelength is $\lambda = 852$ nm. The calculations are based on the Abraham expression for the momentum of light.

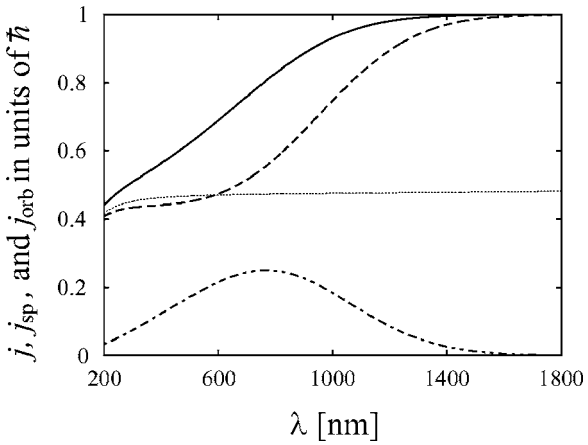

FIG. 3. Total (solid line), spin (dashed line), and orbital (dashed-dotted line) angular momenta per photon in a circularly polarized fundamental mode as functions of the light wavelength. The limiting function $\hbar/n_1^2$ is shown by the dotted line. The fiber radius is $a = 200$ nm. The calculations are based on the Abraham expression for the momentum of light.

nents $\mathcal{E}_0$ and $\mathcal{H}_0$, which contain the harmonic $e^{i\varphi}$, become substantial. Therefore, in the intermediate regime, a substantial orbital angular momentum may appear.

We emphasize that the expressions for $J^{(\mathrm{in})}$ and $J_{\mathrm{sp}}^{(\mathrm{in})}$ given in Eqs. (14) and (18) are valid only in the Abraham formulation. In the Minkowski formulation, we must add an additional factor n_1^2. According to the Minkowski formulation, the angular momentum per photon and its spin and orbital components are given by

$$j^{(\mathrm{M})} = \frac{n_1^2 J^{(\mathrm{in})} + J^{(\mathrm{out})}}{U/\hbar\,\omega},$$

$$j_{\mathrm{sp}}^{(\mathrm{M})} = \frac{n_1^2 J_{\mathrm{sp}}^{(\mathrm{in})} + J_{\mathrm{sp}}^{(\mathrm{out})}}{U/\hbar\,\omega},$$

$$j_{\mathrm{orb}}^{(\mathrm{M})} = j^{(\mathrm{M})} - j_{\mathrm{sp}}^{(\mathrm{M})}. \tag{27}$$

When we use expressions (22) and (23) for the limiting case of thin fibers and expressions (25) and (26) for the limiting case of thick fibers, we can show that $j^{(\mathrm{M})} \cong j_{\mathrm{sp}}^{(\mathrm{M})} \cong \hbar$ and $j_{\mathrm{orb}}^{(\mathrm{M})} \cong 0$ in both limiting cases. Furthermore, our numerical calculations presented in the next section (see Fig. 4) indicate that $j^{(\mathrm{M})} = \hbar$ for any fiber radii. Thus, the Minkowski angular momentum of the guided light is the same as that for the light in free space. This result is consistent with the result of ray optics for the Minkowski angular momentum of a light beam in a semi-infinite dielectric [22].

IV. NUMERICAL RESULTS

In this section, we present results of numerical calculations for the angular momentum and its spin and orbital components for the guided field. We illustrate in Fig. 2 the dependences of j, j_{sp}, and j_{orb} on the fiber radius a. The light wavelength is chosen to be $\lambda = 852$ nm. The corresponding refractive index of the fiber is $n_1 = 1.45$. The refractive index of the vacuum clad is, as already stated before, $n_2 = 1$. The figure shows that $j, j_{\mathrm{sp}}, j_{\mathrm{orb}} \leq \hbar$. When the fiber radius is small, namely $a < 100$ nm, j and j_{sp} approach their maximum value $\hbar$, while j_{orb} tends to zero. We observe that j_{orb} reaches its peak value of about $0.25\hbar$ at $a \cong 222$ nm, and j_{sp} reaches its minimum value of about $0.45\hbar$ at $a \cong 437$ nm. When the fiber radius is large, namely $a > 400$ nm, j_{orb} reduces to zero. In this limit, j and j_{sp} tend to have the same nonzero value, which is estimated to be $\hbar/n_1^2 \cong 0.48\hbar$. Thus, the angular momentum per photon j is in the range from $\hbar$ to $\hbar/n_1^2$. The contribution of the spin component j_{sp} to j is dominant when the fiber radius is small or large compared to the light wavelength. For intermediate fiber radii, a substantial orbital component j_{orb} appears, which is absent in the two limits mentioned above.

Since the dispersion of the fiber material is weak, the normalized fiber size parameter ka is a good approximate scaling parameter. Therefore, the analysis given in the previous section can also be applied to the cases of large and small light wavelengths. We illustrate in Fig. 3 the dependences of j, j_{sp}, and j_{orb} on λ in the case where $a = 200$ nm. As seen, when the light wavelength is large, j and j_{sp} approach their maximum value $\hbar$, but j_{orb} tends to zero. Furthermore, j_{orb} reaches a peak value of about $0.25\hbar$ at $\lambda \cong 768$ nm. When the light wavelength is small, j_{orb} reduces to zero, and j and j_{sp} tend to have the same value $\hbar/n_1^2$. Note that n_1 varies with λ.

The above calculations were based on the Abraham expression for the momentum of light. According to this expression, the angular momentum of a circularly polarized photon in a dielectric medium with the refractive index n_1 is $\hbar/n_1^2$, smaller than the vacuum value $\hbar$ by the factor n_1^2. In the case of a guided mode, each photon is spread both inside and outside the fiber. The characteristic size of the outside part is given by the penetration length of the evanescent wave. It reduces with increasing fiber radius or decreasing light wavelength. This explains why the Abraham angular momentum j of a photon in the guided mode reduces with

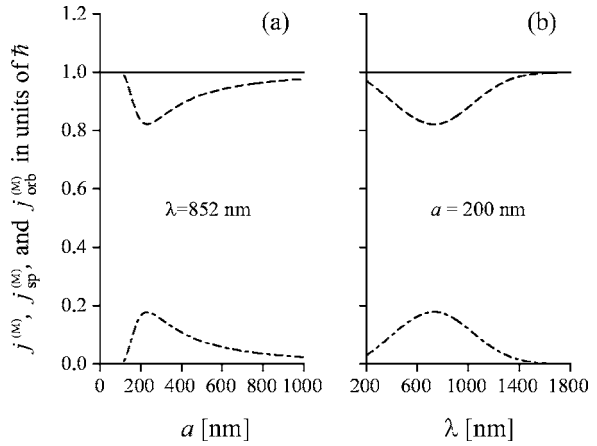

FIG. 4. Calculations from the Minkowski expressions for the total (solid line), spin (dashed line), and orbital (dashed-dotted line) angular momenta as functions of (a) the fiber radius and (b) the light wavelength.

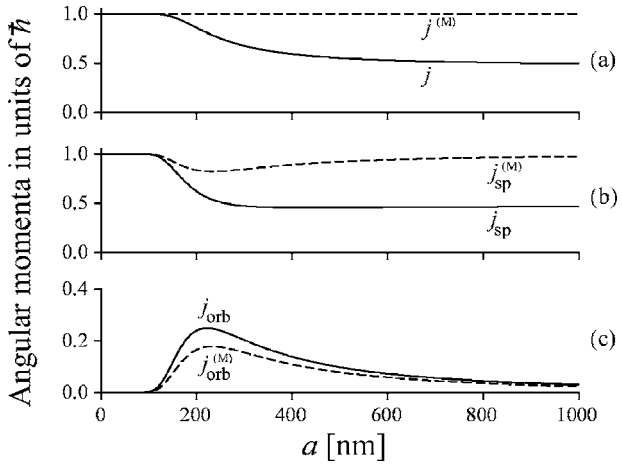

FIG. 5. Comparison between the Abraham (solid lines) and Minkowski (dashed lines) angular momenta per photon of a guided light field. The light wavelength is λ=852 nm.

increasing fiber radius a (see the solid line in Fig. 2) or decreasing light wavelength λ (see the solid line in Fig. 3).

According to the Minkowski expression, the angular momentum of a photon in a dielectric medium is the same as in free space [22]. Although this result was established by ray optics for the field in a semi-infinite dielectric medium, we expect that it remains valid for the field in a guided mode. To check this fact, we plot in Fig. 4 the Minkowski angular momentum $j^{(\mathrm{M})}$ as a function of the fiber radius and the light wavelength. In addition, we also plot the spin component $j_{\mathrm{sp}}^{(\mathrm{M})}$ and the orbital component $j_{\mathrm{orb}}^{(\mathrm{M})}$. The solid lines in the figure confirm that the total Minkowski angular momentum $j^{(\mathrm{M})}$ remains constant and equal to $\hbar$. The dashed lines show that the spin component $j_{\mathrm{sp}}^{(\mathrm{M})}$ reaches its maximum value $\hbar$ in the limits of large and small radii or, equivalently, the limits of small and large wavelengths. The dashed-dotted lines show that, for intermediate radii of the fiber or intermediate wavelengths of the light, a substantial orbital component $j_{\mathrm{orb}}^{(\mathrm{M})}$ appears, which is absent in the limits mentioned above. Similar to the Abraham orbital component j_{orb}, the Minkowski orbital component $j_{\mathrm{orb}}^{(\mathrm{M})}$ has a peak in the region where the fiber radius a is about one-fourth of the light wavelength λ. However, the peak value of $j_{\mathrm{orb}}^{(\mathrm{M})}$ is about $0.18\hbar$, smaller than the peak value of about $0.25\hbar$ of j_{orb}.

To see the difference between the Abraham and Minkowski angular momenta of a guided light field, we plot in Fig. 5 both types of momenta as well as their spin and orbital components as functions of the fiber radius. Figures 5(a) and 5(b) show that $j<j^{(\mathrm{M})}$ and $j_{\mathrm{sp}}<j_{\mathrm{sp}}^{(\mathrm{M})}$, respectively. However, Fig. 5(c) shows that $j_{\mathrm{orb}}>j_{\mathrm{orb}}^{(\mathrm{M})}$. We note that one-half of the difference between the Minkowski and Abraham expressions is sometimes interpreted as the mechanical contribution to the momentum per photon in the field-plus-matter wave [21,22]. Using such an interpretation, we can say that the mechanical contribution to the orbital component [given by $(j_{\mathrm{orb}}^{(\mathrm{M})}-j_{\mathrm{orb}})/2$] is negative while the one for the spin component [given by $(j_{\mathrm{sp}}^{(\mathrm{M})}-j_{\mathrm{sp}})/2$] and the one for the total angular momentum [given by $(j^{(\mathrm{M})}-j)/2$] are positive.

V. SUMMARY

In conclusion, we have shown that light confined in a circularly polarized fundamental mode of a nanofiber has a finite angular momentum, with both spin and orbital components. Using exact solutions of the Maxwell equations for guided modes, we have derived exact analytical expressions for the angular momentum and its spin and orbital components.

We have shown that, in the thin-fiber limit, the Abraham expression for the angular momentum per photon approaches the usual vacuum value $\hbar$, while in the thick-fiber limit it gives the field-only contribution $\hbar/n_1^2$ to the angular momentum of a wave traveling into a dielectric medium. Meanwhile, the Minkowski expression for the angular momentum per photon in the field-plus-matter wave remains constant and equal to $\hbar$ for all fiber radii.

We have found that the spin component is dominant when the fiber radius is small or large compared to the light wavelength. For intermediate fiber radii, a substantial orbital component appears, which is absent in the two limits mentioned above. The orbital component reaches its maximum value of about $0.25\hbar$, according to the Abraham expression, or $0.18\hbar$, according to the Minkowski expression, when the fiber radius a is about one-fourth of the light wavelength λ. By comparing the Abraham and Minkowski expressions, we have found that the mechanical contribution to the orbital part is negative while the mechanical contributions to the spin part and the total angular momentum are positive.

The angular momentum of a light field can be transferred to an atom through the atom-field interaction [3,4]. Such a transfer can influence not only the internal state but also the rotational motion of the atom. It is known that the action of a light beam with a spin angular momentum on an atom is different from that of a light beam with an orbital angular momentum [4]. Since the angular momentum of a circularly polarized guided field has both spin and orbital components, the action of the guided field on an atom is complicated. Unlike the case of light beams in free space, the field in a fiber mode is guided. Therefore, we expect that a nanofiber

carrying a light field that possesses angular momentum can be used for manipulating as well as guiding the rotational motion of atoms. Such issues will be addressed in future work.

Although our study was performed in the Abraham and Minkowski formulations for the momentum of light, it can be easily modified for other formulations. Due to the feasibility and advantages of nanofibers, our work can initiate new experiments to test the validities of different formulations for the momentum of light.

ACKNOWLEDGMENT

This work was carried out under the 21st Century COE program on "Coherent Optical Science."

[1] S. Chu, Rev. Mod. Phys. **70**, 685 (1998); C. Cohen-Tannoudji, *ibid.* **70**, 707 (1998); W. D. Phillips, *ibid.* **70**, 721 (1998).

[2] V. S. Letokhov and V. G. Minogin, *Laser Light Pressure on Atoms* (Gordon and Breach, New York, 1987); A. P. Kazantsev, G. J. Surdutovich, and V. P. Yakovlev, *Mechanical Action of Light on Atoms* (World Scientific, Singapore, 1990).

[3] L. Allen, M. J. Padgett, and M. Babiker, Prog. Opt. **39**, 291 (1999), and references therein.

[4] J. Opt. B: Quantum Semiclassical Opt. **4**, S1 (2002), special issue on atoms and angular momentum of light, edited by L. Allen, H. Rubinsztein-Dunlop, and W. Ertmer.

[5] L. Allen, M. W. Beijersbergen, R. J. C. Spreeuw, and J. P. Woerdman, Phys. Rev. A **45**, 8185 (1992).

[6] L. Allen and M. J. Padgett, Opt. Commun. **184**, 67 (2000).

[7] R. Loudon, Phys. Rev. A **68**, 013806 (2003).

[8] K. Volke-Sepulveda, V. Garces-Chavez, S. Chavez-Cerda, J. Arlt, and K. Dholakia, J. Opt. B: Quantum Semiclassical Opt. **4**, S82 (2002).

[9] S. J. van Enk and G. Nienhuis, Opt. Commun. **94**, 147 (1992); J. Courtial, K. Dholakia, L. Allen, and M. J. Padgett, *ibid.* **144**, 210 (1997).

[10] H. He, M. E. J. Friese, N. R. Heckenberg, and H. Rubinsztein-Dunlop, Phys. Rev. Lett. **75**, 826 (1995).

[11] See, for example, D. Marcuse, *Light Transmission Optics* (Krieger, Malabar, FL, 1989).

[12] V. I. Balykin, K. Hakuta, Fam Le Kien, J. Q. Liang, and M. Morinaga, Phys. Rev. A **70**, 011401(R) (2004); Fam Le Kien, V. I. Balykin, and K. Hakuta, *ibid.* **70**, 063403 (2004).

[13] Fam Le Kien, J. Q. Liang, K. Hakuta, and V. I. Balykin, Opt. Commun. **242**, 445 (2004).

[14] N. Schlosser, G. Reymond, I. Protsenko, and P. Grangier, Nature (London) **411**, 1024 (2001); S. Kuhr, W. Alt, D. Schrader, M. Müller, V. Gomer, and D. Meschede, Science **293**, 278 (2001).

[15] L. Tong, R. R. Gattass, J. B. Ashcom, S. He, J. Lou, M. Shen, I. Maxwell, and E. Mazur, Nature (London) **426**, 816 (2003).

[16] Fam Le Kien, V. I. Balykin, and K. Hakuta, Phys. Rev. A **73**, 013819 (2006).

[17] See, for example, J. D. Jackson, *Classical Electrodynamics*, 3rd ed. (Wiley, New York, 1999).

[18] I. Brevik, Phys. Rep. **52**, 133 (1973).

[19] M. Abraham, Rend. Circ. Mat. Palermo **28**, 1 (1909); **30**, 33 (1910).

[20] H. Minkowski, Nachr. Ges. Wiss. Goettingen, Math.-Phys. Kl. **53**, 42 (1908); Math. Ann. **68**, 472 (1910).

[21] M. Mansuripur, Opt. Express **12**, 5375 (2004); **13**, 2245 (2005); **13**, 5315 (2005).

[22] M. Padgett, S. M. Barnett, and R. Loudon, J. Mod. Opt. **50**, 1555 (2003).

[23] L. Mandel and E. Wolf, *Optical Coherence and Quantum Optics* (Cambridge University Press, New York, 1995), p. 488.